

(see chapters by V. B. Braginsky and D. H. Douglass).

³V. B. Braginsky, *Physical Experiments with Test Bodies* (Nauka, Moscow, 1970) [NASA Report No. NASA-TT F762 (National Technical Information Service, Springfield, Va., 1970), Eqs. (3.17) and (3.25).

⁴R. Giffard, Phys. Rev. D **14**, 2478 (1977).

⁵A simple extension of our argument gives a very general proof of the quantum limit, $T_n \geq \hbar\omega/(k \ln 2)$, on the noise temperature of amplifiers. For a less general proof see H. Hefner, Proc. IRE **50**, 1604 (1962).

⁶V. B. Braginsky, unpublished lectures at California Institute of Technology, Stanford University, Louisiana State University, Massachusetts Institute of Technolo-

gy, and Princeton University.

⁷V. B. Braginsky and Yu. I. Vorontsov, Usp. Fiz. Nauk **114**, 41 (1974) [Sov. Phys. Usp. **17**, 644 (1975)].

⁸The possibility of precise, arbitrarily quick nondestruction measurements was discussed by J. von Neumann, *Mathematische Grundlagen der Quantenmechanik* (Springer, Berlin, 1932), pp. 222-237.

⁹W. G. Unruh, to be published.

¹⁰V. B. Braginsky, Y. V. I. Vorontsov, and F. I. Halili, to be published.

¹¹Actually the condition is $\hat{A}(t_0) = f_1[\hat{A}(t_1)] = \dots = f_n[\hat{A}(t_n)]$, where f_j is an arbitrary real function; but we ignore this trivial generalization.

Measurement of the D Semileptonic Branching Ratio in e^+e^- Annihilation at the $\psi''(3770)$

W. Bacino, A. Baumgarten, L. Birkwood, C. Buchanan, R. Burns,^(a) M. Chronoviat, P. Condon, R. Coombes, P. Cowell,^(b) A. Diamant-Berger,^(c) M. Faessler,^(d) T. Ferguson, A. Hall, J. Hauptman, J. Kirkby, J. Kirz,^(e) J. Liu,^(f) L. Nodulman, D. Ouimette, D. Porat, C. Rasmussen, M. Schwartz, W. Slater, H. K. Ticho, S. Wojcicki, and C. Zupancic^(g)

Stanford Linear Accelerator Center and Physics Department, Stanford University, Stanford, California 94305, and University of California, Los Angeles, California 90024, and University of California, Irvine, California 92664

(Received 31 October 1977)

We have observed the ψ'' resonance in the cross section for $e^+e^- \rightarrow$ hadrons at $E_{c.m.} = 3770 \pm 6.0$ MeV, of total width $\Gamma = 24 \pm 5$ MeV and partial width to electron pairs $\Gamma_{ee} = 180 \pm 60$ eV. The cross section for hadronic events which contain anomalous electron provides both unambiguous evidence of D semileptonic decays and a branching ratio measurement of $(11 \pm 2)\%$.

We report the first results of a SPEAR experiment performed with a new detector DELCO¹ (Fig. 1), designed to identify electrons over 60% of the total solid angle by means of a large atmospheric-pressure Cherenkov counter.

Six concentric cylindrical multiwire proportional chambers (MWPC) extend from the beam pipe to a radius of 30.0 cm. The inner four cylinders subtend 80% of 4π steradians. Azimuthal readout is provided by axial anode wires of 2-mm spacing and crude depth measurement by four cylindrical high-voltage foils divided into 1-cm-wide strips inclined at $\pm 45^\circ$ to the beam axis. The MWPC's are in a 3.5-kG magnetic field provided by two discrete coils wrapped on steel pole pieces 85 cm apart with a return yoke on the outside of the detector. The magnet provides a near-axial field over the MWPC volume, with an average field integral out to the magnetostriuctive wire spark chambers of 1.7 kG m.

Immediately beyond the MWPC the particles enter a twelve-module ethane-filled Cherenkov counter² sensitive only to electrons (π threshold

$= 3.7$ GeV/c). Particles which count by striking the photocathodes are identified by plastic guard counters. Within each module, the Cherenkov light is focused by a 1.5 m \times 1.5 m ellipsoidal mirror via a flat mirror onto a 5-in. RCA 4522

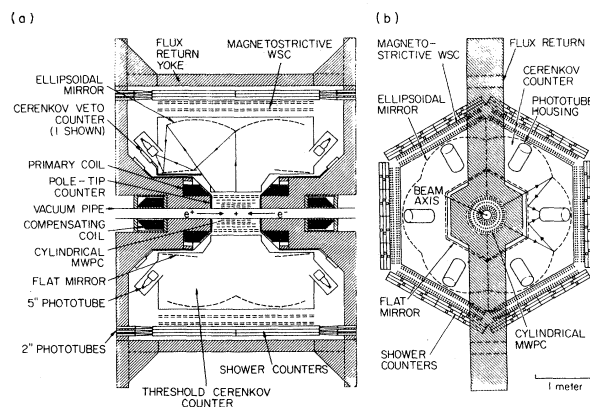


FIG. 1. (a) Polar and (b) azimuthal projections of the apparatus. For illustrative purposes, in (a) the apparatus in the yoke has been rotated by 30° .

phototube coated with pTP (p-terphenyl) wave shifter. The average radiator length of 1 m yields ten photoelectrons for a $\beta = 1$ particle.

Next in each sextant are located two planes of magnetostrictive chambers providing two z and φ measurements per track. Together with the MWPC information they give the following measurement accuracies: $\sigma_p/p = 13p$ (GeV/c)%, $\sigma_\varphi = 5$ mrad and $\sigma_\theta = 4$ mrad.

Finally there is an array of Pb/scintillator shower counters subtending 60% of 4π steradians and consisting of three layers of Pb (6 radiation lengths total) and scintillator. The first layer of scintillator (A counter) is full length and is viewed at each end by a 2-in. phototube. The two following layers are composed of two half-length scintillators, each viewed individually. In addition, the polar region $15^\circ < (\theta, \pi - \theta) < 35^\circ$ is covered by pie-shaped counters attached to the magnet pole tips and read out via blue-green wavelength shifter bars.³ All of the phototube pulses are pulse-height analyzed. All but those on the outer two layers of the shower counters are also time analyzed.

There are four logical components of the trigger: the shower counters, the A counters, the MWPC's, and a beam crossing pulse. A shower counter pulse (S) is defined as a coincidence of at least two of its scintillator layers, permitting relatively soft photons to satisfy S . An A pulse demands the coincidence of signals from tubes at both ends of the scintillator. A logical pulse, γ , is defined by the sum of the signals of all the tubes in the first two layers of shower counters exceeding a threshold set so as to exclude non-showering cosmic rays. A MWPC track (Q_{12}) is defined as a coincidence between two hits in the innermost pair of MWPC cylinders within approximately 3 cm. The beam crossing pulse (X) is derived from a pickup coil near the interaction region and restricts triggers to ± 20 nsec of the beam crossover time.

These components are combined to form three triggers ($C = X \cdot A \cdot 2S \cdot Q_{12}$, $H = X \cdot 2A \cdot 3S$, and $G = X \cdot \gamma \cdot 2S$), with the requirement that shower counters from separate sextants participate. The combined trigger rate is 0.7 Hz.

The raw data comprise typically about 8% Bhabha pairs (e^+e^-) and 5% hadronic events. The remainder are mainly cosmic rays which are removed from the sample by timing cuts (the transit time of cosmic rays is always larger than 11 nsec) and by the requirement that tracks traverse the interaction region.

The integrated luminosity is obtained from the number of detected Bhabha pairs, defined as a pair of tracks in the MWPC deviating from collinearity by no more than 10° with two associated shower counter pulses within ± 3 nsec of the beam-crossing pulse. Furthermore, each electron must be identified either by a shower-counter pulse height ≥ 4 times the pulse height of a minimum-ionizing particle or by a pulse in the appropriate Cherenkov cell (threshold of ~ 0.7 photoelectron).

Triggers are classified as hadronic events if they satisfy all of the following: (a) at least two shower counter pulses within ± 3 nsec of the beam-crossing pulse, (b) at least two visible tracks in the MWPC, (c) vertex near the beam-crossing point, i.e., within ± 10 cm along the beam axis and ± 1 cm perpendicular to the beam axis. Two-track events must satisfy additional criteria: (a) The two tracks are not both identified as e^\pm by Cherenkov and shower-counter pulse height. (b) The tracks are not coplanar with the beam ($\Delta\varphi > 5^\circ$).

Candidates for hadronic events with an e^\pm form that subset of these events in which one of the tracks traverses a Cherenkov cell and a shower counter and both of these given an in-time pulse. To reduce the background from Dalitz pairs, γ conversions, and δ rays, events are not accepted into this sample if the e^\pm track is accompanied by another track within $\Delta\varphi = (15 \text{ GeV mrad})/P$, where P is the momentum of the softer track. This cut has been measured to remove $(15 \pm 5)\%$ of real events. The graphical reconstruction of these events is inspected by physicists in order to eliminate spurious candidates. Approximately 80% of the initial e^\pm hadronic sample pass this final test.

The detection efficiency of Bhabha pairs is easily understood since the topology is simple, radiative losses calculable, and the probability of identifying high-energy electrons inside the fiducial volume excellent ($> 99\%$).

The detection efficiency for hadronic events is calculated by first unfolding the "true" charged-track and photon multiplicity distribution from the observed one, on the assumption of no correlation between the final state products. Once this is known, the overall trigger efficiency is readily obtained by appropriately weighting different final states efficiencies. For events with at least four prongs it is above 90%; and for two-prong events it is $(48 \pm 15)\%$. The overall triggering efficiency at $E_{c.m.} = 3.8$ GeV is 0.85 ± 0.1 where

the error was determined by taking extreme input assumptions compatible with the data. The number of genuine events lost due to misidentification is less than 3% and is comparable to the number of spurious events interpreted as hadrons.

The number of observed hadronic events with electrons has to be corrected for electron losses in the Cherenkov counter due to mirror edges and poor light collection at low momenta. We have measured these inefficiencies with Bhabha events and soft electron pairs from the process $e^+e^- \rightarrow e^+e^-e^+e^-$. These losses amount to 20% when integrated over the observed electron distributions. In addition a small correction is necessary due to absorption of soft electrons in the first Pb layer of the shower counters. This was determined from test-beam data and reaches 15% at 200 MeV.

The measured value of R in the range $3.7 \text{ GeV} < E_{c.m.} < 3.83 \text{ GeV}$ is displayed in Fig. 2(a). The errors shown are statistical and the vertical scale may possess an overall systematic error of $\pm 20\%$. A significant structure is observed⁴ at 3.77 GeV. Figure 2(b) shows the data after removal of the ψ and ψ' radiative tails⁵ [indicated

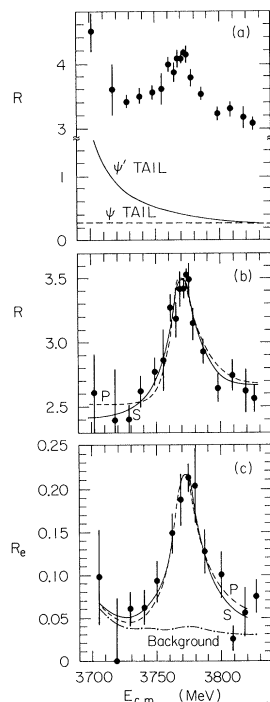


FIG. 2. (a) R as a function of energy; (b) R after subtraction of the radiative tails of ψ and ψ' . The dashed (solid) curve is a P - (S -) wave Breit-Wigner resonance superposed on a background proportional to $P_0^3 + P_+^3 + a$ constant. (c) Plot of R_e , where $R_e = \sigma(e^+e^- \rightarrow e^+ + \geq 2 \text{ charged particles}) / \sigma(e^+e^- \rightarrow \mu^+\mu^-)$.

in Fig. 2(a)]. Since this peak occurs close to D^0 and D^+ thresholds we tried several Breit-Wigner fits with and without dependences on their respective momenta, P_0 and P_+ .⁶ These forms included a resonant S wave or P wave with energy-dependent width superposed on a background term which was either linear or proportional to $P_0^3 + P_+^3$. All of these give resonance parameters which agree within the errors of the fits. Specifically, a P -wave final state with $P_0^3 + P_+^3$ background gave the following: mass, $m = 3770 \pm 6 \text{ MeV}$ (allowing for the energy calibration of SPEAR), $\Gamma = 24 \pm 5 \text{ MeV}$, $\Gamma_{ee} = 180 \pm 60 \text{ eV}$. The error in Γ_{ee} includes $\pm 40 \text{ eV}$ due to the fit and $\pm 40 \text{ eV}$ due to normalization uncertainties. Our values of m and Γ agree with those of Rapidis *et al.*⁴ while our value of Γ_{ee} is less than theirs by a factor of 2. This discrepancy of 0.5 is the product of three factors: 0.8 in the overall scale of the nonresonant hadronic cross section, 0.75 in the height of the resonant peak after correcting by the overall scale factor, and 0.85 in the total width.

The cross section of hadron events with an e^+ and at least two additional prongs is shown in Fig. 2(c). The dot-dashed line is an estimate of the background based on the assumption that there is no anomalous electron production at the ψ or ψ' and derived from the measured probability of observing an electron per hadronic event of $(3.5 \pm 0.3) \times 10^{-3}$ at the ψ and $(8.8 \pm 1.0) \times 10^{-3}$ at the ψ' .⁷ The dashed line shows a P -wave Breit-Wigner fit of the same mass and width as previously determined from the total hadronic cross section.

This resonance can be interpreted as the 3D_1 state of charmonium with $J^{PC} = 1^{--}$ predicted by Eichten *et al.*⁸ at this mass. Its width is two orders of magnitude larger than the $\psi'(3684)$ which indicates that the new state decays almost entirely to pure $D^0\bar{D}^0$ and D^+D^- . Therefore the data of Fig. 2(c) provide unambiguous evidence of D semi-leptonic decays. After correcting the relative size (0.18 ± 0.02) of the peaks in Figs. 2(b) and 2(c) for losses into two and fewer observed prongs (0.20 ± 0.10) we determine a branching ratio of $0.18/(2 \times 0.80) = (11 \pm 2)\%$ for $D \rightarrow e\nu X$. This branching ratio measurement is consistent with those reported⁹ by other e^+e^- experiments.

We would like to thank the Experimental Facilities Division and SPEAR Operation Group for their splendid support of this experiment. This work was supported in part by the U. S. National Science Foundation and the U. S. Department of Energy.

^(a)Current address: Hughes Aircraft, Newport Beach, Calif. 92664.

^(b)Current address: Systems Control, Inc., Palto Alto, Calif. 94302.

^(c)Permanent address: Département de Physique des Particules Élémentaires, Saclay, France.

^(d)Current address: CERN, Geneva, Switzerland.

^(e)Permanent address: State University of New York, Stony Brook, N. Y. 11794.

^(f)Presently with American Asian Bank, San Francisco, Calif.

^(g)Current address: Institute of Nuclear Physics, University of Munich, Munich, West Germany.

¹An acronym of "direct electron counter."

²W. E. Slater *et al.*, to be published.

³We thank Professor B. Barish of California Institute of Technology for providing us with the wavelength-shifter bars.

⁴A parallel observation of this structure has been

made at the SPEAR west interaction region. P. Rapi-dis *et al.*, Phys. Rev. Lett. **39**, 526 (1977).

⁵J. D. Jackson and D. L. Scharre, Nucl. Instrum. Methods **128**, 13 (1975).

⁶J. D. Jackson, Nuovo Cimento **34**, 1645 (1964).

⁷At the ψ' the observed rate is due mainly to $\psi' \rightarrow \psi \pi^+ \pi^- \rightarrow e^+ e^- \pi^+ \pi^-$. At 3.6 GeV, no anomalous electrons were seen in a sample of 470 hadronic events, consistent with the rate measured at the ψ .

⁸E. Eichten *et al.*, Phys. Rev. Lett. **34**, 369 (1975); K. Lane and E. Eichten, Phys. Rev. Lett. **37**, 477, 1105(E) (1976).

⁹A. Barbaro-Galtieri *et al.*, in Proceedings of the International Symposium on Lepton and Photon Interactions at High Energies, Hamburg, August 1977 (to be published); S. Yamada, in Proceedings of the International Symposium on Lepton and Photon Interactions at High Energies, Hamburg, August 1977 (to be published).

Confined Quarks and Analyticity

R. C. Brower and W. L. Spence

Division of Natural Sciences, University of California, Santa Cruz, California 95064

and

J. H. Weis

Department of Physics, University of Washington, Seattle, Washington 98195

(Received 10 November 1977)

We argue that confinement requires singularities in parton-hadron wave functions which are necessary for the parton-model description of physical processes and the analytic structure of hadronic amplitudes. Our arguments are supported by explicit calculations in two-dimensional quantum chromodynamics. In particular, we show, using new WKB techniques, that the amplitudes for $e^- h \rightarrow e^- X$ and $e^+ e^- \rightarrow h X$ are related by analytic continuation in their scaling regions.

A central problem of hadron dynamics is how the "hard" (asymptotic-freedom or parton) properties at short distances can be fused with the "soft" (confinement or dual-Regge) properties of extended hadrons. In this Letter general arguments for some consequences of this fusion are given, supported by calculations in the $1/N_c$ expansion of two-dimensional quantum chromodynamics¹ (QCD₂)—the only model known to possess both "hard"² and "soft"³ physics.

As long as asymptotic freedom is postulated, all the parton properties based on light-cone analysis should be unaffected by confinement. For example, deep inelastic scattering ($\gamma^* h \rightarrow X$) may be calculated *as if* the quarks in the hadron were free. Although confining forces actually cause the formation of hadrons at large distances, the cross section depends only upon the square

of the modulus of the amplitude $\varphi_h^{ai}(x, \vec{k}_\perp)$ for finding a quark of flavor a and momentum ($k_- = xp_-, \vec{k}_\perp$) in the target⁴ [see Fig. 1(a)]. On the other hand, the compatibility of the parton model with confinement is much less clear for processes like inclusive $e^+ e^-$ annihilation ($\gamma^* \rightarrow h X$) in which the observed hadron is produced *after* the quark-antiquark pair have interacted via the confining force.

Despite these physical differences, the amplitudes for $\gamma^* h \rightarrow X$ and $\gamma^* \rightarrow h X$ are expected to be related by analytic continuation⁵ (AC). Thus if $\Phi(x = 1/x_F)$ is defined to be the analytic continuation of $\varphi(x)$ from Bjorken x inside $[0, 1]$ to Feynman $x_F \equiv 1/x$ inside $[0, 1]$, the process $\gamma^* \rightarrow h X$ should be represented by the "crossed handbag" diagram [see Fig. 1(b)], yielding the quark fragmentation function $D_{h/a}(x_F) \propto |\Phi_h^{ai}(1/x_F)|^2$.